JACC Vol. 26, No. 4
October 1995:1080–9

EXPERIMENTAL STUDIES

Cellular Mechanisms of Ventricular Bipolar Electrograms Showing Double and Fractionated Potentials

TAKESHI INO, MD,* MICHAEL C. FISHBEIN, MD, FACC, WILLIAM J. MANDEL, MD, FACC, PENG-SHENG CHEN, MD, FACC, HRAYR S. KARAGUEUZIAN, PHD, FACC

Los Angeles, California

Objectives. **This study sought to determine the types of transmembrane action potentials associated with bipolar electrograms that show double and fractionated potentials.**

Background. **The cellular correlates of ventricular bipolar electrograms showing double potentials and fractionated low amplitude potentials remain poorly defined.**

Methods. **A bipolar electrogram (1-cm interelectrode distance [6F, USCI]) and two transmembrane action potentials (within 1 mm of each pole) were recorded simultaneously in 12 isolated canine right ventricular endocardial preparations (2 × 1 cm, 2 mm thick). The long axis of the bipolar electrode was parallel to the long axis of the superficial endocardial fibers, and the recordings were made at 40 to 500 Hz.**

Results. **The following phenomena were associated with double potentials: 1) an increase in conduction time between the two poles of the bipole during a) the propagation of premature action potentials (7 of 12 tissues in 4 mmol/liter extracellular potassium ion concentration $[K^+]_o$); b) rapid pacing and premature stimuli (3 of 6 in 9 mmol/liter $[K^+]_o$); and c) the propagation of slow responses induced by barium chloride (4 mmol/liter). There was a positive correlation between conduction time (CT) and interspike interval (IPI) of the double potential (IPI [ms] = 0.5 × CT [ms] + 35) during early afterdepolarizations induced by barium chloride (4 mmol/liter) superfusion (three of six tissues). The following events were associated with fractionated electrograms: 1) propagation of induced graded responses (six tissues) in 4 mmol/liter $[K^+]_o$; 2) induced reentry at cycle lengths of 140 to 170 ms in 9 mmol/liter $[K^+]_o$ (four of six tissues); and 3) asynchronous afterdepolarizations induced by 4 mmol/liter barium chloride (four of six tissues).**

Conclusions. **Endocardial double potentials and fractionated electrograms seen on clinically used bipolar electrodes occur under conditions of slowed or discontinuous conduction and induced reentry and during asynchronous automatic firing initiated by afterdepolarizations. Caution must be exercised in interpreting such bipolar electrograms because more than one type of cellular action potential may cause these abnormal electrographic results.**

(J Am Coll Cardiol 1995;26:1080–9)

Bipolar ventricular electrograms showing double potentials (split potentials) and fractionated potentials characterized by multiphasic low amplitude deflections are considered to reflect the presence of an abnormal electrophysiologic substrate at the recording site, both in experimental (1–4) and clinical settings (5–8). It has been suggested (4) that such abnormal electrograms may result from structural abnormalities that occur during the healing phase of myocardial infarction, such as interstitial tissue fibrosis. Alternatively, Spach et al. (9) have indicated that fractionated (polyphasic) electrograms could arise from abnormal cellular transmembrane action potentials that manifest complex and irregular phases of depolarization. It has been further suggested (10) that the extracellular potentials reflect intracellular flow of current. Both double and fractionated potentials have been recorded during sinus rhythm (6,8,11) and during ventricular tachycardia presumed to be caused by reentry (3,5,12). Clinical studies (13) have provided suggestive evidence that these two types of electrograms may result from slow conduction. However, it was not possible in these clinical studies to determine the types of action potentials that may be associated with these abnormal electrograms. In the present study, we sought to determine whether double potentials and fractionated bipolar electrograms occur during 1) slow conduction; 2) spontaneous automatic activity; and 3) reentry in isolated normal endocardial ventricular tissues.

From the Division of Cardiology and Department of Anatomic Pathology, Cedars-Sinai Research Institute and Department of Medicine, University of California Los Angeles School of Medicine, Los Angeles, California. This study was supported in part by the Electrocardiographic Heartbeat Organization (ECHO) of Cedars-Sinai Medical Center, Los Angeles, California and by a grant from the Ralph M. Parsons Foundation, Los Angeles, California; an NIH FIRST Award (HL-50259) and an NIH Specialized Center of Research grant (HL52319), National Heart, Lung, and Blood Institute, National Institutes of Health, Bethesda, Maryland; and an American Heart Association National Center Grant-in-Aid (92009820), Dallas, Texas.

Manuscript received October 7, 1994; revised manuscript received April 25, 1995, accepted May 5, 1995.

*Present address: Division of Cardiology, Nippon Medical School, Tokyo, Japan.

Address for correspondence: Dr. Hrayr S. Karagueuzian, Cedars-Sinai Medical Center, Davis Research Building, Room 6066, 8700 Beverly Boulevard, Los Angeles, California 90048.

0735-1097/95/$9.50
0735-1097(95)00256-4

Methods

Tissue isolation. Ten adult male and female mongrel dogs weighing between 15 and 22 kg were anesthetized with intravenous sodium pentobarbital (30 to 35 mg/kg body weight). After a left lateral thoracotomy, the hearts were rapidly removed and immediately placed in oxygenated cold Tyrode's solution. Twelve endocardial tissue samples (2 × 1 cm, 2 mm thick) were dissected near the outflow tract from the 10 isolated right ventricles and were mounted and pinned, endocardial surface upward, in a tissue bath. To avoid tissue complexity, care was taken not to include any trabecular muscle bundles or small twigs of free-running Purkinje fibers. The epicardial portion of the isolated tissue block was trimmed and discarded to reduce the thickness of the tissue down to 1.5 to 2 mm. All tissue samples were superfused at a constant rate of 8 ml/min with normal Tyrode's solution saturated with 95% oxygen, 5% carbon dioxide. The composition of the Tyrode's solution was (mmol/liter) as follows: sodium chloride 135, potassium chloride 4.5, sodium dihydrogen phosphate 1.8, calcium chloride 2.7, magnesium chloride 0.5, sodium bicarbonate 24 and dextrose 5.5, in triple-distilled deionized water. The temperature of the tissue bath was maintained at 37 ± 0.2°C (mean ± SD) and the pH at 7.4 ± 0.1. The tissue preparations were paced with a custom-made constant-current programmable stimulator (14) at a current strength of twice the diastolic excitability threshold through Teflon-coated (except at the tip) bipolar silver wires (0.1 mm in diameter) placed 0.25 mm apart placed on the tissue surface. A bipolar catheter electrode with an interelectrode distance of 10 mm (6F, USCI) was gently placed on the endocardial surface parallel to the endocardial fiber orientation. Histologic studies showed (see later) that the most superficial (40 to 60) endocardial cell layers ran parallel from the base to the apex.

Recording arrangements. Two transmembrane action potentials were recorded simultaneously, each within 1 mm of each of the two poles of the bipolar electrode (Fig. 1). Transmembrane action potentials were recorded through a machine-pulled glass capillary microelectrode filled with 3 mol/liter potassium chloride with a tip resistance of 15 to 30 MΩ (14). The action potentials were recorded from the most superficial (first three) cell layers, which could be either a Purkinje fiber or a ventricular muscle cell. The stimulating electrode was placed within 2 mm of the "proximal" pole of the bipolar electrode catheter (Fig. 1). Extracellular electrograms obtained through the bipolar electrode were coupled to an alternating current amplifier with filter frequencies of 40 to 500 Hz, as is routine in clinical electrophysiologic studies (5–8). Both microelectrode and bipolar recordings were displayed on a multichannel oscilloscopic-photographic recorder (E for M, DR-16) and photographed at a paper speed of 50 to 200 mm/s. Before the start of each experiment, all isolated tissue blocks were equilibrated in the tissue bath for 40 to 60 min.

Protocol of stimulation and recordings. In six endocardial preparations, the effects of incremental pacing rates at cycle

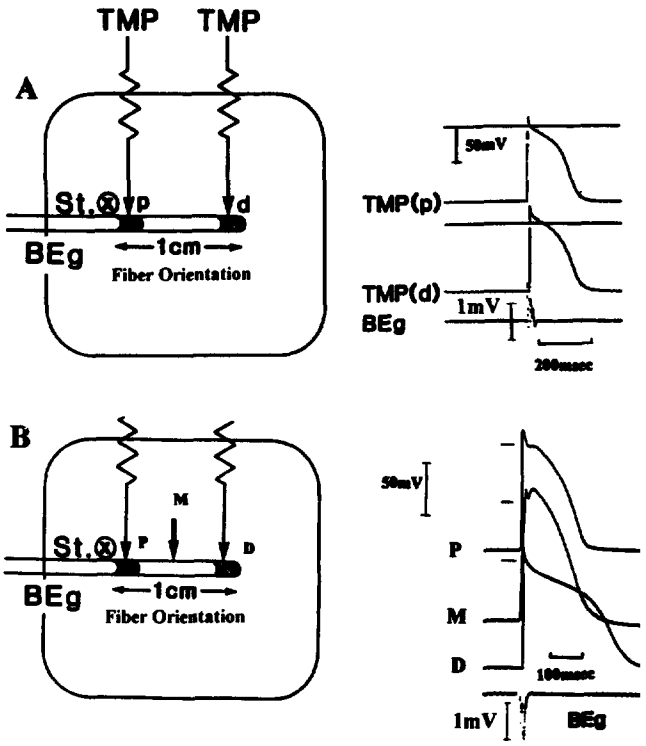

Figure 1. Diagram of microelectrode recording arrangements of transmembrane action potentials (TMP) and bipolar electrograms (BEg). **Panel A (left)** shows the position of the 6F USCI bipolar electrogram relative to fiber orientation, proximal (p) and distal (d) to the stimulating electrode (St.). **Panel A (right)** shows three simultaneous recordings from their respective sites (**left**). **Panel B** shows four simultaneous recordings: three (**top**) microelectrodes and one 6F USCI bipolar electrogram (**bottom**). The third microelectrode recording is from the middle (M) of the recording bipolar electrode. In **panel A**, transmembrane action potential recordings from the proximal and the distal sites are from Purkinje fibers. In **panel B,** transmembrane action potential recordings at the proximal (P) and middle sites are from ventricular muscle cells and that at the distal (D) site is from a Purkinje fiber. Note that the polarities of the deflections of the bipolar electrograms in the two tissues are different; however, the activation sequence (from proximal to distal sites) and conduction time (6 to 8 ms) are comparable in the two tissues.

lengths of 800 to 200 ms and that of premature stimuli were evaluated during an increase in the Tyrode's solution extracellular potassium ion concentration ($[K^+]_o$) from 4.5 to 9 mmol/liter for 45 to 60 min. Single premature stimuli (S_2) were delivered after 9 regular beats at cycle lengths of 400 to 800 ms, at progressively shorter coupling intervals until refractoriness was reached. Double and triple premature stimuli (S_3 and S_4) were also applied during similar basic drives, after fixing S_2 and S_3 10 ms outside the effective refractory periods of S_1 and S_2, respectively. In the remaining six preparations, after initial control recordings during superfusion with normal Tyrode's solution, the tissues were superfused with Tyrode's solution containing 4 mmol/liter barium chloride for 30 to 45 min. In these six tissues we studied the effects of barium-induced automaticity in the form of spontaneous phase 4 depolarization and early afterdepolarizations, as described

previously (15–17). The conduction time between the proximal and distal cells was measured by the time lapse between the fast upstrokes of the two action potentials recorded within 1 mm of each pole. After the termination of these studies, all tissues were superfused with normal Tyrode's solution for 45 to 60 min to reverse (washout) the effects of the various interventions.

Histologic studies. At the conclusion of the electrophysiologic studies, all tissue samples were fixed in 10% neutral buffered formaldehyde and stored in a refrigerator. Six-micrometer sections were made perpendicular to the endocardial surface to detect the presence, if any, of autolytic tissue changes in deeper myocardial cells. Another six-micrometer section, parallel to the base–apex axis, was also made to determine the myocardial fiber orientation at the site of bipolar electrogram recordings. Three to five sections were made in each tissue preparation, and each section was stained with hematoxylin-eosin (18).

Definitions. *Double potentials* are defined as two spikes or two voltage deflections during a single beat that are separated by a low amplitude baseline or by an isoelectric interval. *Fractionated potentials (electrograms)* are defined as multiple low amplitude (<1 mV) potentials during a given beat that are not separated by an isoelectric interval.

Statistical analysis. Linear regression analysis was performed to correlate the interpotential interval of a double potential with conduction time and conduction velocity and to correlate the duration of the bipolar electrograms with the conduction time between the two microelectrodes. Data across several cycle lengths were compared first using repeated measure analysis of variance and then multiple paired comparisons. A p value <0.05 was considered significant. Results are presented as mean value ± SD.

Results

Action potential propagation in subendocardial cardiac fibers. During regular drive, at a 800-ms cycle length with normal Tyrode's superfusion, the mean conduction time between the two poles of the bipolar electrode (1 cm), measured as the time lapse between the fast upstrokes of the two action potentials, was 6.3 ± 2.3 ms (range 5 to 8) (Fig. 1). This value corresponds to an average linear conduction velocity of 158 cm/s. The sequential nature of the propagation of action potentials from proximal to distal ("linear") through the most superficial endocardial cardiac fibers was verified by recording in four experiments a third action potential from the middle of the two poles of the bipolar electrode (5 mm away from each recording site) and demonstrating that the activation in the middle occurs after the proximal and before the distal activation (Fig. 1, panel B). The subendocardial Purkinje fiber network covers the entire right ventricular endocardial surface with a depth up to four cell layers thick (18). However, at certain sites the recordings from the most superficial cell layer were characteristic of ventricular muscle cells, not of Purkinje fibers. The nature of the cell types recorded at the proximal or distal sites, or both, had no effect either on the sequence of activation or on the conduction time between the two poles of the bipolar electrode (compare panels A and B in Fig. 1).

Double potentials. Double potentials were induced when the conduction velocity between the two poles of the bipole was reduced to <50 cm/s either during rapid pacing or when multiple (up to three) premature extrastimuli were applied. Double potentials on the bipolar electrograms were seen during the following three interventions:

1. Effects of rapid pacing and premature stimulation in normal Tyrode's solution. Rapid pacing and single premature stimulation did not result in either conduction slowing or in a change in the configuration of the bipolar electrograms (Fig. 2, A). However, when double (S_3) and triple (S_4) premature stimuli were applied at short coupling intervals (range 115 to 128 ms, mean 120 ± 8), conduction velocity was slowed to levels <50 cm/s (Fig. 2). When such conduction slowing occurred, splitting of the bipolar electrogram potential was observed in 7 of 12 tissue samples studied. The interval between the spikes increased as the conduction velocity between the two poles further decreased (Fig. 2). In three tissue samples, the application of S_4 at still shorter coupling intervals (i.e., at 115 and 110 ms) caused conduction block to the distal microelectrode recording site (Fig. 2, C). The distally blocked impulse was associated with the disappearance of the second deflection of the double potential electrogram (Fig. 2, C). The two upstrokes of the action potentials coincided in time with the two deflections of the double potential electrogram.

2. Effects of rapid pacing and premature stimulation in 9 mmol/liter $[K^+]_o$. Superfusion of the endocardial tissues (n = 6) with high potassium concentrations (9 mmol/liter) caused a significant ($p < 0.05$) reduction in the membrane rest potential of both Purkinje fibers (from 81.2 ± 7.2 to 73.7 ± 6.7 mV) and ventricular muscle cells (from 78.5 ± 8.4 to 74.6 ± 6 mV), with a concomitant shortening of the action potential duration (from 263.6 ± 20.1 to 201.28 ± 28.5 ms for Purkinje fibers; from 195.7 ± 28.6 to 155.5 ± 32.6 ms for ventricular muscle cells) and refractoriness (from 225.7 ± 12.5 to 198.5 ± 12.8 ms for Purkinje fibers; from 161.8 ± 11.6 to 101.5 ± 9.8 ms) for muscle cells. These changes, observed during the 800-ms cycle length of stimulation, were consistent with previous studies (19). Rapid pacing and premature stimulation in tissues superfused with 9 mmol/liter $[K^+]_o$ caused the appearance of double potentials in three of the six tissue samples studied. In the remaining three tissue samples, rapid pacing caused continuous, fractionated electrograms (see later). Figure 3 shows the emergence of double potentials during faster pacing rates. Note that the distal action potential is preceded by a low amplitude (3 to 6 mV) prepotential that precedes the fast upstroke of the action potential. In two tissue samples progressive increase in the stimulation frequency resulted in a greater slowing of the conduction velocity caused by a step delay (prepotential) in the distal cell (Fig. 3). The effects of the 9 mmol/liter potassium superfusion were promptly reversed after 45 min of superfusion with Tyrode's solution containing 4 mmol/liter $[K^+]_o$.

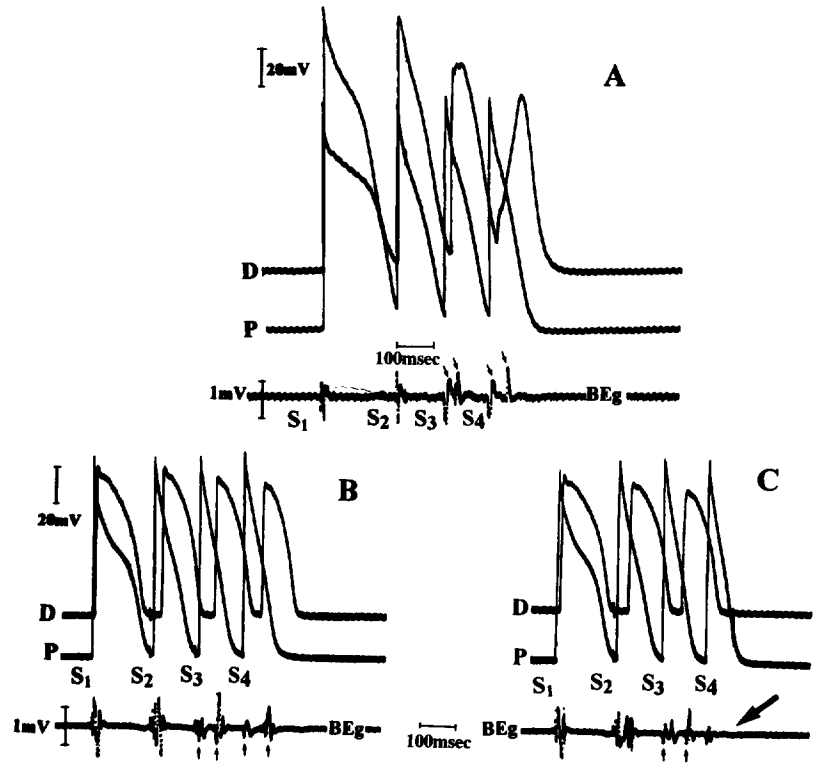

Figure 2. Effects of multiple premature stimuli on conduction time and bipolar electrogram configuration in endocardial tissue superfused with Tyrode's solution containing 4 mmol/liter $[K^+]_o$. Proximal (P) and distal (D) are transmembrane action potential recordings, as shown in Figure 1. **A,** A single premature stimulus (S_2) has no effect on proximal to distal conduction time and on the configuration of the bipolar electrogram (BEg). The second (S_3) and third premature stimuli (S_4), however, were associated with conduction slowing of 20 and 50 ms, respectively, causing splitting of the bipolar electrogram into two discrete deflections **(small arrows)**. Note that each deflection coincided in time with the two upstrokes of the action potential. **B,** S_2 caused a 20-ms conduction time between the proximal and the distal recording sites and a lengthening of the bipolar electrogram duration from 20 to 35 ms. However, conduction times during S_3 and S_4 were increased to 45 and 55 ms, respectively, causing splitting of the bipolar electrogram **(small arrows)** with interspike intervals of 40 and 55 ms, respectively. **C,** The premature coupling interval of S_4 was decreased from 135 ms **(panel B)** to 125 ms, resulting in distal conduction block of S_4. Distal block of S_4 was associated with the disappearance of the second deflection of the bipolar electrogram **(large arrow)** in **panel C.** S_1 = regular pacing at 400-ms cycle length. Tissue samples in **B** and **C** are different from that in **A.** See Figure 1 for details.

3. Effects of 4 mmol/liter barium chloride. In six tissues samples, 4 mmol/liter barium chloride superfusion induced partial depolarization from a mean rest potential of 81 ± 4 to 56 ± 7 mV (n = 12 cells). Although these preparations generated early afterdepolarizations causing spontaneous activity, transient periods (3 to 5 min) of quiescence often ensued in four tissue samples, allowing regular drive cycle lengths of 400 to 500 ms. The regular drive permitted us to evaluate the

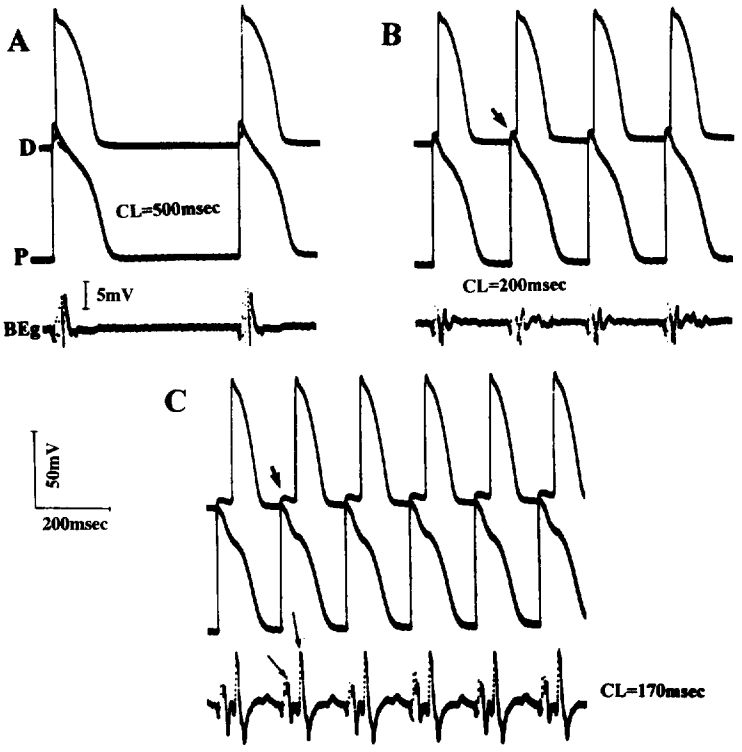

Figure 3. Rapid pacing and induction of prepotentials and double potentials in endocardial ventricular tissue sample superfused with Tyrode's solution containing 9 mmol/liter $[K^+]_o$. Distal cell action potential is preceded by a prepotential **(single arrow)**, the interval of which increases with decreasing the cycle lengths (CL) of stimulation from 500 ms **(A)** to 200 ms **(B)** to 170 ms **(C)**. Double potentials of the bipolar electrogram are apparent in **C,** where each deflection of the double potential coincides in time with the proximal (P) and distal (D) upstrokes of the two action potentials. See Figure 1 for details.

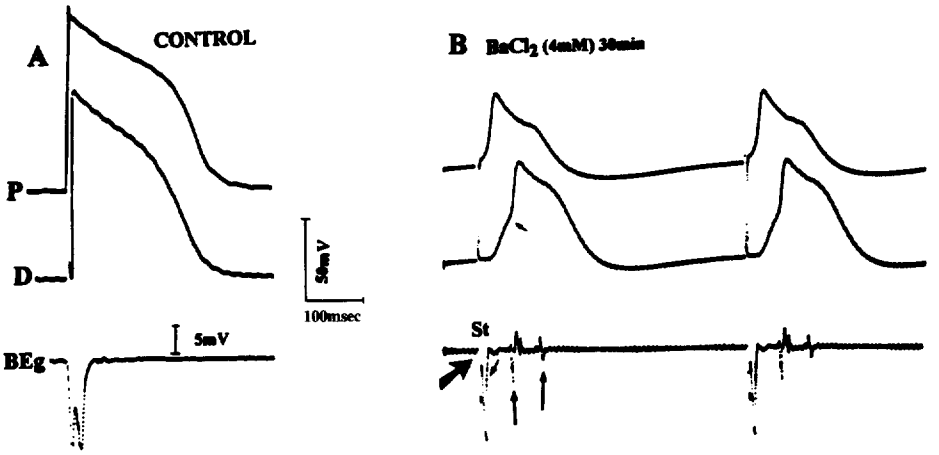

Figure 4. Effects of barium-induced slow-response action potentials and double potentials on the bipolar electrogram (BEg). The tissue is paced regularly at a 450-ms cycle length. Note that the distal cell action potential is preceded by a prepotential (**small arrow [B]**). Each deflection of the bipolar electrogram double potentials (**small arrow** after the large stimulus artifact [St, **large arrow**] and **small downward-pointed arrow**) coincide in time with the proximal (P) and distal cell (D) upstrokes. The third small deflection on the bipolar electrogram (**right arrow**) may reflect step-delayed distant activation at an adjacent site. See Figure 1 for details.

effects of slow conduction caused by slow-response action potentials on the bipolar electrogram configuration. The excitability of the barium chloride-treated tissues was decreased, requiring 8 to 10 times stronger current (i.e., 2 to 5 mA). Figure 4 illustrates an example of barium chloride-induced partial depolarization in an endocardial tissue preparation that was regularly driven at a 500 ms cycle length. The cells in these tissues had the characteristics of slow-response fibers and showed various degrees of stimulus response latencies (60 to 100 ms) with very slow upstrokes. Propagation of the impulses was from the proximal to the distal recording site (Fig. 4, B), as was the case during the pre–barium chloride state (Fig. 4, A). The velocity of the conduction in the slow-response fibers was reduced from 125 cm/s (fast response) to ~10 cm/s, with a mean conduction velocity of 12.5 ± 4.3 cm/s in the four tissue samples studied. Such severe conduction slowing was associated with the appearance of double potentials on the bipolar electrogram (Fig. 4, B). The two upstrokes of the proximal and the distal cell action potentials coincided in time with the two deflections of the double potentials. The third small deflection on the electrogram may have resulted from a delayed activation at an adjacent site. In three tissues treated with barium chloride, bouts of spontaneous automatic activity apparently caused by single early afterdepolarizations were associated with double potentials (Fig. 5). The double potentials in these cases emerged by a mechanism that was clearly independent of the conduction time between the proximal and distal cells. The proximal and distal cells initiated action potentials simultaneously (action potential numbers 3 and 4, Fig. 5, B), yet the bipolar electrogram showed double potentials. Barium chloride–induced double

Figure 5. Barium-induced early afterdepolarizations, spontaneous activity and double potentials on the bipolar electrogram (BEg). Note early afterdepolarizations (action potentials 3, 4 and 5) both on the proximal (P) and distal cells (D) and double potentials on the bipolar electrogram (**double arrows [B]**). The proximal and distal cells fire spontaneously, and the observed double potentials on the bipolar electrogram cannot be correlated with an orderly conduction slowing between the two cells. No clear-cut correlation between bipolar electrogram and the automatic activity recorded with the two microelectrodes can be made. For example, action potential 4 of the distal cell manifests an "aborted" early afterdepolarization (**arrow**) that may reflect activity at some distance from the distal cell. The bipolar electrogram recorded with action potentials 3 and 4 shows double potentials.

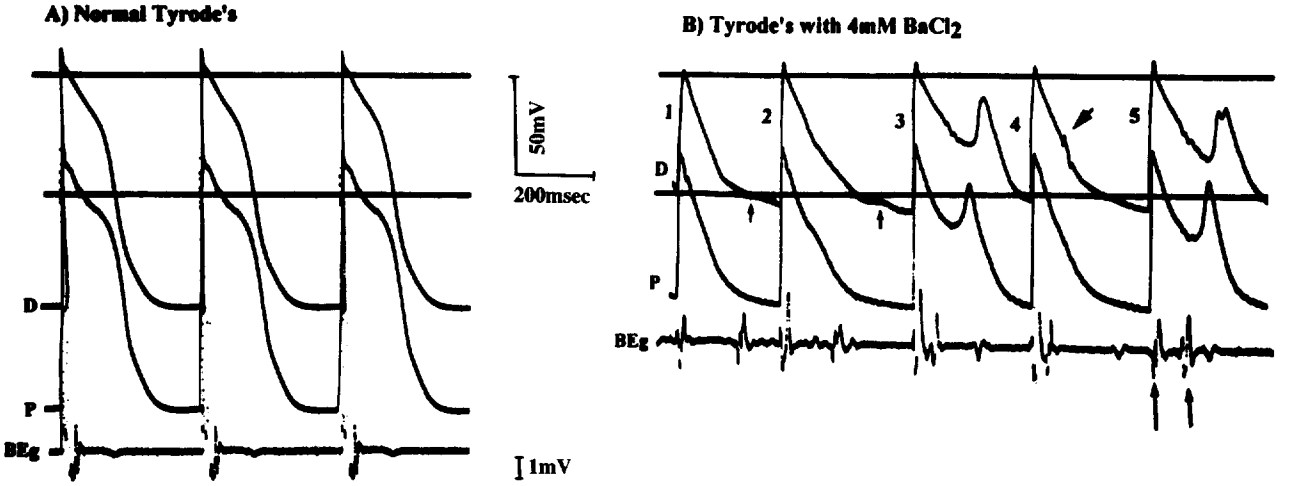

potentials were reversed after 60 min of washout with barium chloride–free Tyrode's solution, whereas the effects on the transmembrane potentials were only partially reversed.

Regression analysis of conduction versus interpotential interval. Regression analysis between the conduction velocity or conduction time and the interpotential interval of the double potentials (pooled data of 30 episodes) showed a significant linear correlation ($p < 0.01$) between these two variables, with a correlation coefficient of 0.58 and 0.65, respectively (Fig. 6): Interpotential interval (ms) = 70.7 − 0.41 × Conduction velocity (cm/s); and Interpotential interval (ms) = 35 + 0.50 × Conduction time (ms) (Fig. 6).

Fractionated electrograms. *Normal Tyrode's solution containing $[K^+]_o$.* In six tissue samples superfused with Tyrode's solution containing 4 mmol/liter $[K^+]_o$, neither rapid pacing nor single premature stimulation could induce fractionation of the bipolar electrogram. Conduction time between the proximal and the distal microelectrode recording sites remained between 5 and 8 ms.

Effects of 9 mmol/liter $[K^+]_o$. A significant increase in conduction time occurred at all cycle lengths (800 to 200 ms) of stimulation during 9 mmol/liter $[K^+]_o$ superfusion. Conduction time increased from 5.6 ± 1.2 to 10.6 ± 3.1 ms at the 800-ms pacing cycle length and from 7.5 ± 2 to 27.6 ± 175 ms at the 200-ms cycle length ($p < 0.05$). In three of the six tissue samples, the bipolar electrogram became fractionated (spikes ranging from 0.1 to 0.4 mV), with a net total prolongation of its duration at all cycle lengths of stimulation ($p < 0.05$). Regression analysis between conduction time and total duration of the bipolar electrogram (15 episodes) showed a significant linear correlation ($p < 0.05$) between these two variables with a correlation coefficient of 0.74: Conduction time (ms) = 0.35 × Bipolar electrogram duration (ms) + 3.18.

Graded responses in 4 mmol/liter $[K^+]_o$. The application of premature stimuli with 4 to 10 times diastolic current threshold during the relative refractory period (i.e., ~50 ms shorter than the effective refractory period) induced "local" responses (n = 6), also known as "graded responses" as originally coined by Weidmann (20). Figure 7 illustrates an example of two induced graded responses with S_2 and S_3 stimuli in a proximal Purkinje

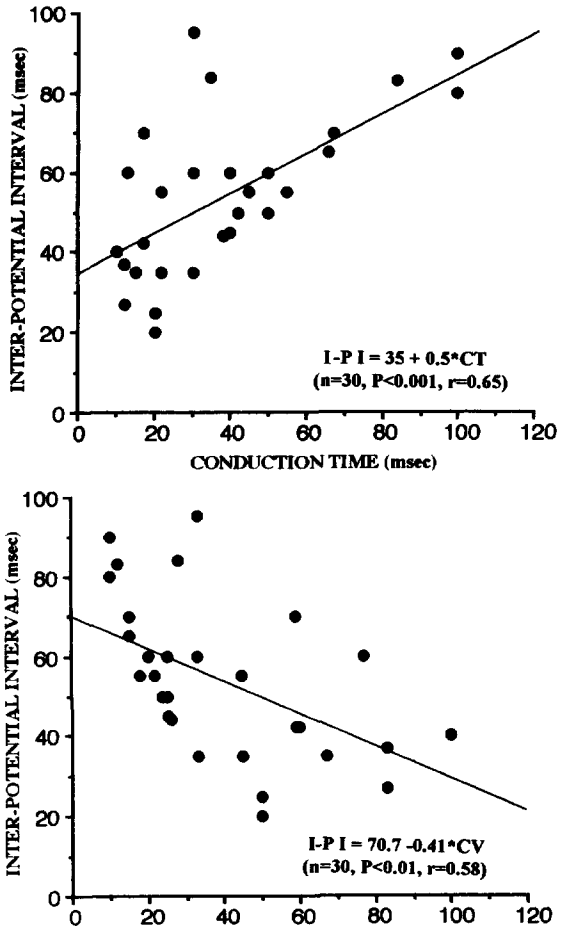

Figure 6. A plot of the interpotential interval (I-P I) versus conduction time (CT) (**top**) and conduction velocity (CV) (**bottom**). Data (**circles**) are pooled from 30 different measurements in 10 tissue samples. **Diagonal lines** = regression lines.

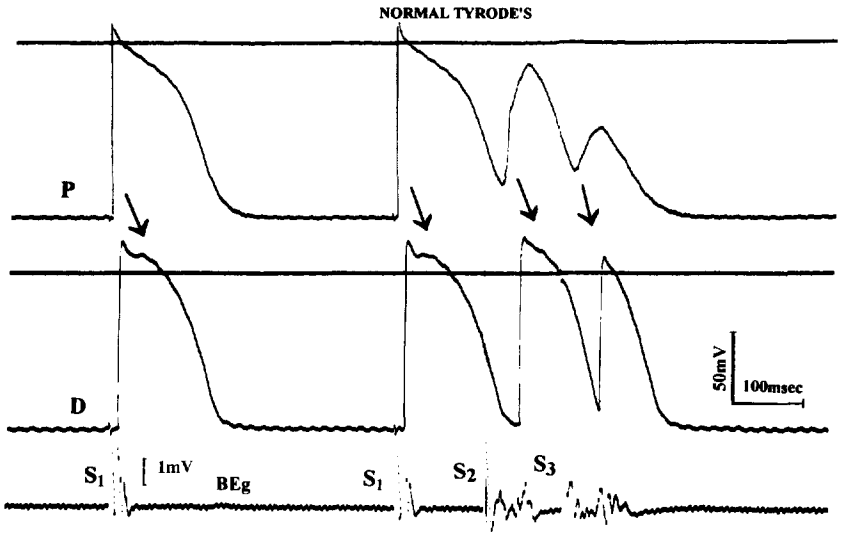

Figure 7. Propagating graded responses induced by premature stimuli (S_2 and S_3) applied at 122- and 114-ms coupling intervals, respectively, in a tissue superfused with normal Tyrode's solution. Propagation of full-height action potentials (first and second action potentials) and the graded responses (third and fourth responses) occurs from the proximal (P) to the distal (D) cell (**arrows**). Note that propagation of the graded responses and not that of the full-height action potentials is associated with fractionation of the bipolar electrogram (BEg). S_1 = regular pacing at 400-ms cycle length.

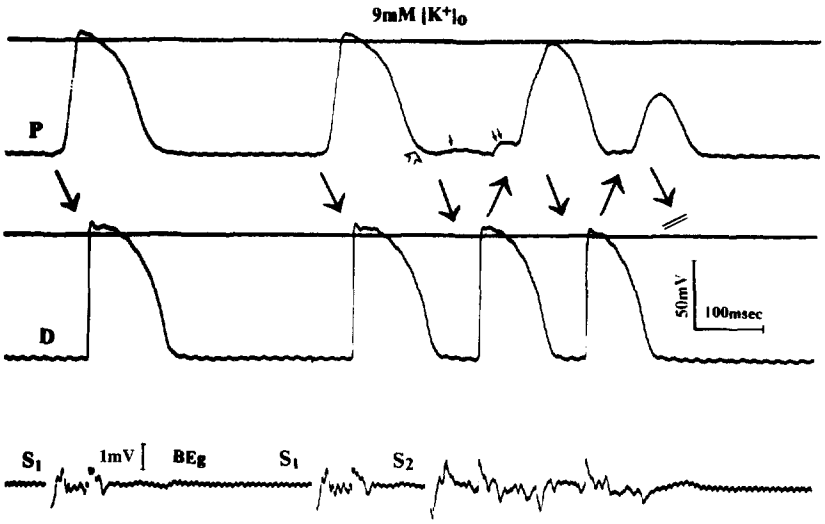

Figure 8. Induction of reentry with propagating graded responses and fractionation of the bipolar electrogram (BEg) during superfusion with Tyrode's solution containing 9 mmol/liter $[K^+]_o$. A premature stimulus (S_2) at a coupling interval of 170 ms **(open arrow)** induces a graded response near the proximal (P) cell **(single small arrow)** that propagates slowly to the distal (D) cell and initiates an action potential at site D after 75 ms compared with 52 ms during regular stimulation at 400 ms (first and second action potential pairs). The distally originated action potential then propagates retrogradely to the proximal cell and initiates an action potential preceded by a prepotential **(double small arrows)**. This activity then propagates to the distal cell and initiates the second action potential in the distal ventricular muscle cell, which in turn propagates again retrogradely and initiates a graded response in the proximal cell. This graded response then blocks **(short double-diagonal lines)** and terminates reentry. Reentry and the propagation of the graded responses are associated with fractionation of the bipolar electrogram. S_1 = regular pacing at 400-ms cycle length; **large arrows** = direction of propagation.

fiber that propagated to the distal recording site. These graded response have been shown earlier (21) and more recently by us (22) to propagate (for up to 6 mm away from the stimulus site) and initiate a regenerative response at the distal recovered cells when the graded response amplitude assumes a threshold value in these recovered cells. Because the ventricular muscle cell refractory period is shorter than that for the Purkinje fibers, the distally propagated graded responses may encounter fully recovered ventricular muscle cells and thus initiate an action potential. Figure 7 illustrates an example in which the S_2- and S_3-induced propagated graded responses initiate full action potentials in the distal recovered ventricular muscle cells. The mean proximal to distal conduction time of the graded responses was 45 ± 6 ms (n = 5) rather than 5 ± 2 ms ($p < 0.05$). In all six tissues, the propagation of the induced graded responses from the proximal cell toward the distal cell was associated with fractionation of the bipolar electrogram (Fig. 7).

Graded responses and reentry: effects of 9 mmol/liter $[K^+]_o$. We tested the hypothesis that shortening the refractory period by superfusion with Tyrode's solution containing 9 mmol/liter $[K^+]_o$ would cause the distally originated action potentials (induced by the propagating graded responses) to return to the proximal site and initiate an action potential as a "reentrant" beat. Figure 8 illustrates an example of an S_2-induced distal origination of an action potential by propagating graded response (small arrow). The induced-graded response near the stimulus site was adjacent to the proximal impaled cell. The distally initiated action potential then propagates slowly to the proximal site and initiates an action potential at this site that is preceded by a prepotential (Fig. 8, small double arrows). The distally initiated action potential then propagates back to the proximal cell with a considerable delay (100 ms) and initiates an action potential at the proximal recovered cell, which in turn propagates to the distal cell to initiate a graded response. The distally induced graded response then blocks reentry (Fig. 8, double line), resulting in the termination of the "reentrant" activity (Fig. 8A). Reentry was associated with fractionation of the bipolar electrogram, which abruptly terminated on termination of reentry. We were able to induce reflected reentrant activity in four of the six tissues studied with 9 mmol/liter $[K^+]_o$.

Barium chloride–induced early afterdepolarizations. Superfusion with 4 mmol/liter barium chloride caused partial depolarization and initiation of spontaneous repetitive activity by the mechanisms of early afterdepolarizations and spontaneous phase 4 depolarization (abnormal automaticity) in all six endocardial preparations studied. Figure 9 illustrates a representative experiment in which three simultaneous action potentials were recorded, each showing its own rate and rhythm. Bipolar electrograms recorded during these early afterdepolarizations showed continuous, low amplitude fractionated activity. The effects of barium chloride were partially reversed after 60 min of superfusion with barium chloride–free Tyrode's solution. During the barium chloride washout, the rate of automatic activity decreased, and isoelectric intervals became more apparent on the bipolar electrogram, as was the case during the early phases of barium chloride effects (Fig. 9, B).

Myocardial fiber orientation. In all 12 tissue preparations, histologic examination showed that the most superficial cell layers (up to a depth of 70 cell layers) had myocardial fibers that were longitudinally oriented from base to the apex. The line connecting the proximal to the distal cell (recording axis) was confirmed microscopically to be parallel to the long axis of the superficial fiber orientation. There were no foci of necrosis

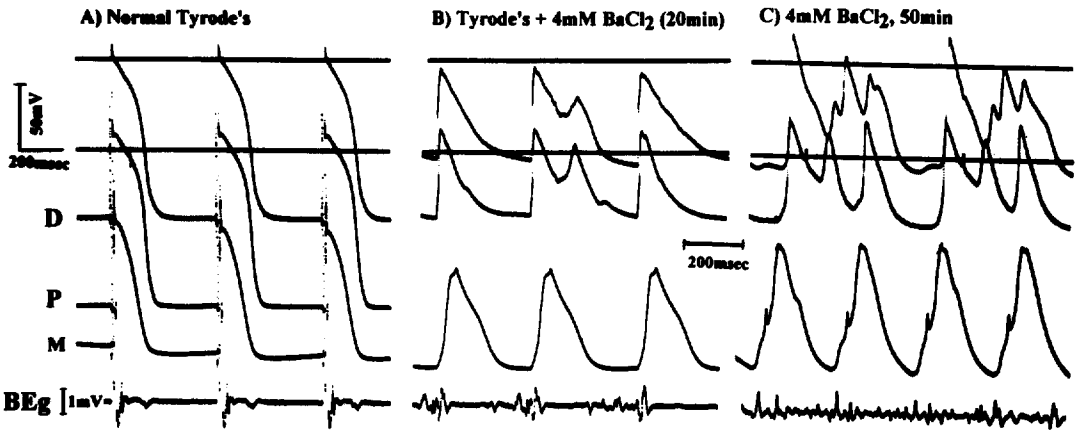

Figure 9. Fractionated bipolar electrogram (BEg) activity during early afterdepolarizations and spontaneous repetitive activity induced by barium chloride. Three simultaneous action potential recordings and a bipolar electrogram were made, as shown in Figure 1, panel B. Increased frequency of early afterdepolarizations and spontaneous activity (**C**) were associated with continuous fractionation of the bipolar electrogram, which was absent during control recordings (**A**) and during the first 20 min of barium chloride exposure (**B**).

or autolytic tissue changes in the deeper myocardial cell layers. The angle formed between the long axis of the fiber orientation and the recording axis was between 0° and 9°, with a mean of 5 ± 2° in the 12 tissue samples.

Discussion

Our ability to record endocardial ventricular double and fractionated potentials associated with different types of cellular action potentials constitutes the main finding of the present report. The 6F USCI bipolar electrode used in the present study is often used in clinical studies for endocardial recordings. The characteristics of these electrograms were comparable to our previously reported studies (23) using similar tissue preparations. It has been argued (7,24) that fractionated electrograms might be caused by movement artifact. Our 2-mm thick tissues pinned to the floor of the bath showed no visible movement, thereby eliminating movement at the electrode–tissue interface as a possible cause of electrogram fractionation.

Mechanisms of double potentials. Both slow conduction and early afterdepolarizations were associated with double potentials. The interpotential interval was positively correlated with conduction time between the two poles of the bipole, even though this relation was not always very exact. A lack of precise coincidence in time between the upstrokes of the action potentials and the deflections of the bipolar electrogram was also observed in normal ventricular specialized conducting tissue (25) and in slow-response atrioventricular node cells (26), a phenomenon that may result when the location of the recorded cellular activity is at some distance from the poles of the bipolar electrogram. In the present study the close proximity of the cellular action potential recordings to the poles of the bipolar electrode often caused the proximal and distal upstrokes of the action potentials to coincide in time with the two deflections of the bipolar double potentials. The presence of small additional deflections on the electrogram (Fig. 4) may result from asynchronous activation at an adjacent site. Such asynchrony may result from a step delay in conduction, as evidenced by the presence of foot potentials in the distal trace. These prepotentials may conceivably be caused by an increase in intracellular calcium ion concentration ($[Ca^{2+}]_i$) during barium chloride and high $[K^+]_o$ superfusion. Increased $[Ca^{2+}]_i$) may promote reversible increase in junctional resistance (27), which in turn may then cause prepotentials in cells just distal to a region of high resistance by electrotonic interaction (28–31).

Double potentials were also observed during barium chloride–induced spontaneous asynchronous automatic activity induced by early afterdepolarizations. During such asynchronous (multiple automatic foci) activity, no orderly (proximal to distal) conduction slowing can be expected; therefore the observed double potentials could arise by the mechanism of early afterdepolarizations independent of conduction alterations. The transient and irregular nature of these double potentials may reflect the asynchronous nature of this type of cellular automatic activity. However, we cannot be certain whether each of the two deflections of the double potentials results from the observed early afterdepolarizations at the proximal and distal cells. In fact, double potentials were observed on the bipolar electrogram when neither cell generated an early afterdepolarization. In such instances an early afterdepolarization could have arisen in adjacent cells and caused electrogram deflection by an electrotonic interaction. Clinical studies have suggested that double potentials can be recorded during either atrial (32,33) or ventricular tachycardia (34) and also during normal sinus rhythm (35). It therefore appears that double potentials may be caused by more than one mechanism. Early afterdepolarizations and slow or discontinuous conduction appear to be two potential mechanisms of double potentials.

Fractionated electrograms. The range of the voltage amplitude and the duration of the multiphasic fractionated elec-

trograms recorded in the present study were comparable to those seen in clinical studies (5–8). We used a bipolar electrode configuration (6F, USCI) that is routinely used in clinical electrophysiologic studies. However, smaller electrodes with shorter distances between the poles have been associated with a shorter duration of the fractionated electrograms (4). Therefore, it would appear that larger interelectrode distances could record over a larger area of tissue and thus may manifest a longer duration of fractionated activity (36). When discontinuous and slow propagation occurs, the bipolar electrogram may manifest fractionation because the summation of the extracellular currents underlying the bipolar potentials occurs at disparate times, a phenomenon that may cause fractionation (4). We do not know why slowing of the conduction causes a fractionated electrogram in some tissue samples and double potentials in others. It is possible that the discontinuous nature of the slowly propagating wavefront along the axis of the bipolar electrode may be more heterogeneous (i.e., encounters a greater number of intercellular junctions or higher intercellular resistance barriers, or both) in some tissue samples than in others. When intercellular resistance and tissue complexities increase, the disparity (asynchrony) in the activation times during the slowly propagating wavefront might result in fractionation of the electrogram. Lesh et al. (37) showed that the same increase in intercellular resistance that causes slowing of conduction might also be associated with double potentials and fractionated electrograms both in computer simulation and in isolated tissue. Reentry induced by strong premature stimuli (8 to 10 times diastolic threshold currents) were also associated with fractionated electrograms in open chest anesthetized dogs (38). These relatively strong stimuli induce propagating graded responses that cause distal origination of the action potential in recovered cells, as originally described by van Dam et al. (21). The distally initiated action potentials then propagate to the proximal recovered cells and initiate an action potential at this proximal site, causing fractionation of the electrogram. Because we did not map activation with multiple recordings, we cannot be certain whether the retrogradely propagating action potentials occurred through the same fibers (true reflection) or through other fibers (circus movement reentry).

Limitations of the study. The primary objective of the present study was to determine the types of ventricular endocardial action potentials recorded adjacent to bipolar electrodes that showed double and fractionated potentials after (acute [i.e., changes in ionic composition]) interventions. These wave form shapes did not occur until the acute interventions were introduced. This approach required the use of isolated in vitro endocardial tissue preparations with their inherent limitations because such an approach in the in situ ventricle is extremely difficult if not impossible. One such limitation may be the restricted diffusion of nutrients in the in vitro superfused preparations ~1 mm in depth from the surface (39). Because our tissue preparations were in the range 1.5 to 2 mm, it could be argued that the deeper myocardial cells receive lesser amounts of nutrients than do the most superficial cells, leading to tissue autolysis in the deeper cells. This result might then lead to fractionation as a result of asynchronous tissue activation. The absence of autolytic changes in the core of the tissue, as verified microscopically at the end of each study, along with the reversibility of the ionic interventions refute these potential metabolic limitations as a cause abnormal electrographic results.

Clinical implications. With clinically used standard bipolar electrode catheters (6F, USCI), one can record double potentials and fractionated potentials under conditions of slow conduction, asynchronous automatic and reentrant activities. It is suggested that when such bipolar electrograms are recorded from patients, caution be exercised in their interpretation because multiple types of cellular action potentials might be associated with these abnormal electrographic results. For a reliable clinical–experimental correlation, it is important that both poles of the bipole touch the ventricular myocardium because floating of one of the poles in the ventricular cavity may invalidate such correlation. In addition, in many patients fractionated and double potentials may result from nonuniform tissue anisotropy with normal individual cell action potential properties. In such patients, abnormal wave forms may be produced by the loss of side-to-side connections between individual fibers or groups of fibers with normal action potentials.

We thank Avile McCullen, AA for excellent technical assistance.

References

1. Waldo AL, Kaiser GA. A study of ventricular arrhythmias associated with acute myocardial infarction in the canine heart. Circulation 1973;47:1222–8.
2. Boineau JP, Cox JL. Slow ventricular activation in acute myocardial infarction. A source of re-entrant premature ventricular contractions. Circulation 1973;48:702–13.
3. El-Sherif N, Scherlag BJ, Lazzara R, Hope RR. Re-entrant ventricular arrhythmias in the late myocardial infarction period. 2. Patterns of initiation and termination of re-entry. Circulation 1977;55:702–19.
4. Gardner PI, Ursell PC, Fenoglio JJ, Wit AL. Electrophysiologic and anatomic basis for fractionated electrograms recorded from healed myocardial infarcts. Circulation 1985;72:596–661.
5. Josephson ME, Horowitz LN, Farshidi A. Continuous local electrical activity. A mechanism of recurrent ventricular tachycardia. Circulation 1978;57:659–65.
6. Cassidy DM, Vassallo JA, Buxton AE, Doherty JU, Marchlinski FE, Josephson ME. The value of catheter mapping during sinus rhythm to localize site of origin of ventricular tachycardia. Circulation 1984;69:1103–11.
7. Waxman HL, Sung RJ. Significance of fragmented ventricular electrogram observed using intracardiac recording techniques in man. Circulation 1980; 62:1349–56.
8. Klein H, Karp RB, Kouchoukos NT, Zorn GL, James TN, Waldo AL. Intraoperative eletrophysiologic mapping of the ventricles during sinus rhythm in patients with a previous myocardial infarction. Identification of the electrophysiologic substrate of ventricular arrhythmias. Circulation 1982;66: 847–53.
9. Spach MS, Barr RC, Johnson EA, Kootsey JM. Cardiac extracellular potentials: analysis of complex wave forms about the Purkinje networks in dogs. Circ Res 1973;33:465–83.
10. Spach MS, Miller WT, Miller-Jones E, Warren RB, Barr RC. Extracellular potentials related to intracellular action potentials during impulse conduction in anisotropic canine cardiac muscle. Circ Res 1979;45:188–204.
11. Weiner I, Mindich B, Pitchon R. Fragmented endocardial electrical activity

in patients with ventricular tachycardia: a new guide to surgical therapy. Am Heart J 1984;107:86–97.

12. De Bakker JMT, Coronel R, Tasseron S, et al. Ventricular tachycardia in infarcted, Langendorff-perfused human heart: role of the arrangement of surviving cardiac fibers. J Am Coll Cardiol 1990;15:1594–607.
13. Stevenson WG, Weiss JN, Wiener I, et al. Fractionated endocardial electrogram associated with slow conduction in humans: evidence from pace-mapping. J Am Coll Cardiol 1989;13:369–76.
14. Kobayashi Y, Peters W, Khan SS, Mandel WJ, Karagueuzian HS. Cellular mechanisms of differential action potential duration in canine ventricular muscle cells during single vs double premature stimuli. Circulation 1992;86: 955–67.
15. Reid JA, Hecht JJ. Barium induced automaticity in right ventricular muscle in the dog. Circ Res 1967;21:849–56.
16. Mugelli A, Amerini S, Piazzesi G, Giotti A. Barium-induced spontaneous activity in sheep cardiac Purkinje fibers. J Mol Cell Cardiol 1983;15:697–712.
17. Ino T, Karagueuzian HS, Hong K, Meesmann M, Mandel WJ, Peter T. Relation of monophasic action potential recorded with contact electrode to underlying transmembrane action potential properties in isolated cardiac tissue. A systematic microelectrode validation study. Cardiovasc Res 1988; 22:255–64.
18. Sugi K, Karagueuzian HS, Fishbein MC, Mandel WJ, Peter T. Cellular electrophysiological characteristics of surviving subendocardial fibers in chronically infarcted right ventricular myocardium susceptible to inducible sustained ventricular tachycardia. Am Heart J 1987;114:559–69.
19. Hoffman BF, Cranefield PF. The Electrophysiology of the Heart. New York: McGraw-Hill, 1960:91–4; 186–90.
20. Weidmann S. Effects of current flow on the membrane potential of cardiac muscle. J Physiol 1951;115:227–36.
21. van Dam RT, Moore NE, Hoffman BF. Initiation and conduction of impulses in partially depolarized cardiac fibers. Am J Physiol 1963;204:1133–44.
22. Gotoh M, Chen P-S, Mandel WJ, Karagueuzian HS. Graded responses and induction of ventricular rotors by a premature stimulus [abstract]. Circulation 1993;88(pt 2):I–626.
23. Karagueuzian HS, Kobayashi Y, Khan SS, et al. Action potential alternans and irregular dynamics during quinidine intoxication in ventricular muscle cells. Implications to proarrhythmias. Circulation 1993;87:1661–72.
24. Ideker RE, Lofland GK, Smith WM, et al. Late fractionated potentials and continuous electrical activity caused by electrode motion. PACE 1993;6:908–14.
25. Myerburg RJ, Nilsson K, Zoble RG. Relationship of surface electrogram recordings to activity in the underlying specialized conduction tissue. Circulation 1972;45:420–32.
26. De Bakker JMT, Coronel R, Mcguire MA, et al. Slow potentials in the atrioventricular junctional area of patients operated on for atrioventricular node tachycardias and in isolated porcine hearts. J Am Coll Cardiol 1994;23:709–15.
27. De Mello WC. Effects of intracellular injection of calcium and strontium on cell communication in heart. J Physiol 1975;250:231–45.
28. Wennemark JR, Ruesta VJ, Brody DA. Microelectrode study of delayed conduction in the canine right bundle branch. Circ Res 1968;23:753–69.
29. Antzelevitch C, Jalife J, Moe GK. Characteristics of reflection as a mechanism of reentrant arrhythmias and it relationship to parasystole. Circulation 1980;61:182–91.
30. Weingart R, Maurer P. Action potential transfer in cell pairs isolated from adult rat and guinea pig ventricles. Circ Res 1988;63:72–80.
31. Joyner RW. Effects of discrete pattern of electrical coupling on propagation through an electrical syncytium. Circ Res 1982;50:192–200.
32. Cosio FG, Arribas F, Barbero JM, Kallmeyer C, Goicolea A. Validation of double-spike electrograms as markers of conduction delay or block in atrial flutter. Am J Cardiol 1988;61:775–80.
33. Feld GK, Shahandehrad F. Mechanism of double potentials recorded during sustained atrial flutter in the canine right atrial crush-injury model. Circulation 1992;86:628–41.
34. Olshansky B, Moreira D, Waldo AL. Characterization of double potentials during ventricular tachycardia. Studies during transient entrainment. Circulation 1993;87:373–81.
35. Olshansky B, Okumura K, Henthorn RW, Waldo AL. Characterization of double potentials in human atrial flutter: studies during transient entrainment. J Am Coll Cardiol 1990;15:833–41.
36. Karagueuzian HS and Wit AL. Studies on ventricular arrhythmias in animal models of ischemic heart disease. What can we learn? In: Kulbertus HE, Wellens HJJ editors, Sudden Death. The Hague: Martinus Nijhoff, 1980:69–88.
37. Lesh MD, Spear JF, Simson MB. A computer model of the electrogram: what causes fractionation? J Electrocardiol 1988;Suppl:S69–S73.
38. Euler DE, Moore EN. Continuous fractionated electrical activity after stimulation of the ventricles during the vulnerable period: evidence for local reentry. Am J Cardiol 1980;46:783–91.
39. Gibbs CL. Cardiac energetics. Physiol Rev 1978;58:174–254.